

k·p theory of semiconductor superlattice electronic structure in an applied magnetic field

G. Y. Wu* and T. C. McGill

Thomas J. Watson, Sr. Laboratory of Applied Physics, California Institute of Technology, Pasadena, California 91125

C. Mailhot

Xerox Corporation, Webster Research Center (0114-41D), 800 Phillips Road, Webster, New York 14580

D. L. Smith

Los Alamos National Laboratory, Los Alamos, New Mexico 87545

(Received 21 July 1988)

We present a $\mathbf{k}\cdot\mathbf{p}$ theory of semiconductor superlattices in an applied magnetic field. We consider superlattices with a [001] growth axis and the magnetic field along the growth axis. A single-basis set for the constituent materials is provided by a zone-center pseudopotential calculation with a reference Hamiltonian. The Γ_{15} valence and Γ_1 conduction states are coupled with a spinor and treated explicitly. Nearby energy states are treated in Löwdin perturbation theory with the $\mathbf{k}\cdot\mathbf{p}$ operator and the difference between the material pseudopotential and the reference pseudopotential as the perturbation. The calculation is carried out consistently to first order in wave functions and second order in energies. Magnetic, exchange (in semimagnetic materials), spin-orbit, and strain (in strained-layer superlattices) interactions are included between the explicitly included states. When inversion-asymmetry and warping terms are dropped in the Hamiltonian, a Landau index becomes a good quantum number. Bloch and evanescent states are computed for a fixed Landau index in each material. Interface matching of the constituent-material bulk eigenfunctions is accomplished with use of results derived for the normal component of the current density operator. The Landau indices are not mixed by the interface matching. Superlattice translational symmetry is used to derive an eigenvalue equation for the superlattice wave vectors and eigenfunctions. The numerical implementation of the formal results is described and used to investigate a nonmagnetic superlattice $\text{Ga}_{0.47}\text{In}_{0.53}\text{As}/\text{Al}_{0.48}\text{In}_{0.52}\text{As}$ and a semimagnetic superlattice $\text{Hg}_{0.95}\text{Mn}_{0.05}\text{Te}/\text{Cd}_{0.78}\text{Mn}_{0.22}\text{Te}$.

I. INTRODUCTION

Magneto-optical and magnetotransport experiments are very useful in studying the band-edge properties of semiconductors.¹⁻⁴ In order to interpret the results of such measurements, it is necessary to have a detailed theory of the effect of magnetic fields on the band-edge states. In bulk semiconductors, ($\mathbf{k}\cdot\mathbf{p}$) theory has been successful in interpreting the results of magneto-optic and magnetotransport measurements. In Refs. 5 and 6 a detailed ($\mathbf{k}\cdot\mathbf{p}$) theory of direct-band-gap semiconductor superlattices was presented. In this theory the ($\mathbf{k}\cdot\mathbf{p}$) interaction and the difference in one-electron potentials between the two constituent materials making up the superlattice were consistently included through second order. The purpose of this paper is to extend the results of Refs. 5 and 6 to include the effects of an applied magnetic field. Previous work on the magnetic response of superlattices⁷⁻¹² has been performed using the envelope-function approximation and therefore bears the same relation to this work that envelope-function approximation calculations without a magnetic field bear to Refs. 5 and 6. (See the discussion in Appendix V of Ref. 5.)

A magnetic field couples to both the orbital motion and the spin of the carriers. For nonmagnetic semiconductors, the orbital motion coupling is usually more important. We also consider superlattices in which one or

both of the constituent materials are semimagnetic^{13,14} such as (Cd,Mn)Te. In this case, there is also a strong exchange coupling between the band-edge carriers and the d levels of the magnetic ion (Mn). In bulk materials this exchange interaction is usually treated by using a virtual crystal approximation to handle the random positions of the magnetic ions in the alloy and a mean-field theory to describe the spin state of the magnetic ions.^{13,14} We use both approximations here to describe semimagnetic superlattices. We assume that parameters describing the average spin state of the magnetic ion as a function of magnetic field and temperature, which are determined in bulk materials are also appropriate in the superlattice. When the exchange interaction is treated using these two approximations, it looks the same as the direct coupling of the magnetic field to the carrier spins. It greatly increases the size of the spin splittings produced by the magnetic field, but it does not change the symmetry of the problem. The virtual-crystal approximation and mean-field theory have been largely successful in describing the magnetic response of carriers in bulk semimagnetic semiconductors.^{13,14} One of our goals is to describe the magnetic response of carriers in superlattices at the same level of approximation as has been used, and proved largely successful, to describe the magnetic response of carriers in bulk semiconductors.

In Ref 5 a complex band structure is calculated for the

bulk of each constituent material making up the superlattice. Matching of the bulk Bloch and evanescent states at the superlattice interfaces is accomplished using results derived about the normal component of the current density operator. Wave vector parallel to the plane of the superlattice interfaces is a conserved quantity in the wavefunction matching. The superlattice translational symmetry is used to derive an eigenvalue equation for superlattice wave vectors and eigenfunctions. Application of a magnetic field changes the bulk Hamiltonians and thus the complex band structures calculations. We consider [001] growth axis superlattices with the magnetic field orientated along the growth axis. Parallel wave vector is no longer a good quantum number for the bulk Hamiltonian with an applied magnetic field. With the magnetic field along the growth axis, one component, depending on the gauge choice, of the parallel wave vector is a good quantum number. If two classes of small terms are dropped in the bulk Hamiltonian, a Landau index also becomes a good quantum number. This approximation is usually made in describing the magnetic response of carriers in bulk semiconductors and we use it here. We then calculate a complex band structure for each constituent material making up the superlattice. The method of performing this complex-band-structure calculation is the same as in Ref. 5 although the results are different because of the applied magnetic field. The magnetic field does not change the interface matching conditions. The component of parallel wave vector which is a good bulk quantum number is conserved in the interface matching. Neglecting some very small terms in the current density expressions, the Landau index is also conserved in the interface matching. The superlattice translational symmetry along the growth axis is used to derive an eigenvalue equation for superlattice wave vectors normal to the interfacial planes and eigenfunctions much as was done for the case without an applied magnetic field. Thus the treatment of the superlattice in the presence of a magnetic field generally follows that without a magnetic field although there are a number of important differences. We have previously presented the results of some calculations^{15,16} based on the method we now describe.

The paper is organized in the following way. In Sec. II we present the formal theoretical results; in Sec. III, the numerical implementation of these results is described and examples of superlattice magnetic response for a nonmagnetic superlattice and a semimagnetic superlattice are presented; and in Sec. IV, we summarize our conclusions. Explicit expressions for the Hamiltonian are given in the Appendix.

II. FORMAL RESULTS

In this section we generalize the formal results of Ref. 5 to include a magnetic field applied along the growth axis. Those parts of the theory which are essentially the same as in Ref. 5 will be described only briefly. This section is divided into three parts: A, the description of the constituent materials; B, the interface matching; and C, the superlattice eigenvalue equation.

A. Description of the constituent materials

As in Ref. 5, we define a reference Hamiltonian by

$$H_R = \frac{P^2}{2m} + \frac{1}{2} [V^a(r) + V^b(r)], \quad (1)$$

where a and b label the constituent materials and $V^l(r)$ is the pseudopotential of material l described in terms of pseudopotential form factors. The reference Hamiltonian is solved at the Brillouin-zone center, in terms of a plane-wave basis, to give a set of energies and cell periodic, zone center, eigenfunction, ϵ_β and $U_\beta(r)$. The zone-center eigenfunctions provide a single-basis set which will be used to describe the states in both of the constituent materials. We divide the set of states U_β into two groups. One group consists of the threefold Γ_{15} valence-band states and the Γ_1 conduction-band state each combined with a spinor. These eight states are treated explicitly. We use the notation U_d , where d runs over the eight states, to label them. The other spatial states, also combined with a spinor, form the second group of states. These states will be included through first order in the wave function in Löwdin perturbation theory.¹⁷ The perturbation consists of $(\Delta V^l + \mathbf{K} \cdot \mathbf{P}/m)$, where ΔV^l is the difference between the pseudopotential of material l and the reference pseudopotential and

$$\hbar \mathbf{K} = \left[\mathbf{P} + \frac{e}{c} \mathbf{A} \right], \quad (2)$$

where \mathbf{A} is the vector potential. We take

$$\mathbf{A} = -By\hat{x}, \quad (3a)$$

so that

$$\mathbf{B} = B\hat{z}, \quad (3b)$$

where B is the magnitude of the magnetic field. The wave functions in each material take the form¹⁸

$$\psi_\alpha = \sum_d C_d^\alpha \left[f_d^\alpha(r) U_d(r) + \sum_\beta \left[\frac{\left[\mathbf{P} + \frac{e}{c} \mathbf{A} \right] f_d^\alpha(r) \cdot \langle U_\beta | \mathbf{P} | U_d \rangle}{m(\epsilon_d - \epsilon_\beta)} + \frac{f_d^\alpha(r) \langle U_\beta | \Delta V | U_d \rangle}{(\epsilon_d - \epsilon_\beta)} \right] U_\beta(r) \right], \quad (4)$$

where $f_d^\alpha(r)$ is normalized in the sample volume, α is a quantum number, and $C_d^\alpha f_d^\alpha(r)$ satisfies¹⁹

$$\begin{aligned} & \sum_d \left[\epsilon_d \delta_{dd'} + \left[\mathbf{P} + \frac{e}{c} \mathbf{A} \right] \cdot \mathbf{D} \cdot \left[\mathbf{P} + \frac{e}{c} \mathbf{A} \right] + \left[\mathbf{P} + \frac{e}{c} \mathbf{A} \right] \cdot \mathbf{W} + \langle U_{d'} | \Delta V | U_d \rangle \right. \\ & \quad \left. + \sum_\beta \left[\frac{\langle U_{d'} | \Delta V | U_\beta \rangle \langle U_\beta | \Delta V | U_d \rangle}{(\epsilon_d + \epsilon_{d'})/2 - \epsilon_\beta} \right] + \left\langle U_{d'} \left| H_{s.o.} + H_{st} + H_e + \frac{e\hbar}{2mc} \mathbf{B} \cdot \boldsymbol{\sigma} \right| U_d \right\rangle \right] C_d^\alpha f_d^\alpha(r) = E_\alpha C_d^\alpha f_d^\alpha(r). \end{aligned} \quad (5a)$$

Here

$$\mathbf{D} = \frac{1}{2m} \delta_{dd'} + \frac{1}{m^2} \sum_\beta \frac{\langle U_{d'} | \mathbf{P} | U_\beta \rangle \langle U_\beta | \mathbf{P} | U_d \rangle}{(\epsilon_d + \epsilon_{d'})/2 - \epsilon_\beta} \quad (5b)$$

and

$$\mathbf{W} = \langle U_{d'} | \mathbf{P} | U_d \rangle + \sum_\beta \left[\frac{\langle U_{d'} | \mathbf{P} | U_\beta \rangle \langle U_\beta | \Delta V | U_d \rangle}{(\epsilon_d + \epsilon_{d'})/2 - \epsilon_\beta} + \frac{\langle U_{d'} | \Delta V | U_\beta \rangle \langle U_\beta | \mathbf{P} | U_d \rangle}{(\epsilon_d + \epsilon_{d'})/2 - \epsilon_\beta} \right], \quad (5c)$$

$H_{s.o.}$ is the spin-orbit interaction, H_{st} is the strain interaction in strained-layer superlattices, and H_e is the exchange interaction. We take^{13,14}

$$H_e = \sum_j J(\mathbf{r} - \mathbf{R}_j) \mathbf{S}_j \cdot \boldsymbol{\sigma} \quad (6a)$$

$$\rightarrow \mathbf{x} \left[\sum_i J(\mathbf{r} - \mathbf{R}_i) \right] \langle \mathbf{S} \rangle \cdot \boldsymbol{\sigma}, \quad (6b)$$

where $J(\mathbf{r} - \mathbf{R}_j)$ is the exchange integral, j sums over sites of the magnetic ions, x is the concentration of the magnetic ions, i sums over cation sites (assuming that the magnetic ion sits on a cation site), and $\langle \mathbf{S} \rangle$ is the ensemble average of the magnetic ion spin. The mean-field and virtual-crystal approximations, which are expressed in Eq. (6b), neglect clustering of the magnetic ions at the superlattice interfaces. We take the ensemble average of the magnetic ion spin and matrix elements of the exchange interaction summed on cation sites to be given by bulk alloy values. As a result, they are constant in each superlattice layer. These approximations are appropriate for superlattices whose layers are thick compared to the range of the exchange interaction. The exchange interaction only appears for semimagnetic materials.

Equations (4) and (5) are the usual $\mathbf{k} \cdot \mathbf{p}$ equations describing a bulk semiconductor in a magnetic field except for the terms containing ΔV . These terms arise because the basis states here are determined by the reference pseudopotential rather than the material's pseudopotential. The term proportional to ΔV in Eq. (4) corresponds to the first-order correction to the periodic function U_d . The terms proportional to ΔV and $(\Delta V)^2$ in Eq. (5a) correspond to first- and second-order corrections to the energy ϵ_d . These terms will be diagonal. The terms proportional to ΔV in Eq. (5c) correspond to first-order corrections to the first-order momentum matrix element. (There is only one such distinct matrix element, between the Γ_1 and Γ_{15} states. Momentum matrix elements between the threefold degenerate Γ_{15} states vanish.) Only first-order corrections appear in Eq. (5c), because the term itself is already first order in the $(\mathbf{k} \cdot \mathbf{p}/m)$ interaction. Notice that there are no ΔV corrections to the

second-order matrix elements in Eq. (5b) because these terms are already second order in the $(\mathbf{k} \cdot \mathbf{p}/m)$ interaction. Therefore, these terms are the same in the two constituent materials making up the superlattice. The terms containing ΔV do not complicate the solution of the bulk Hamiltonian.

Equation (5) is the same as Eqs. (6) and (7) of Ref. 5 except for the terms containing \mathbf{A} , the exchange term H_e , and the spin term proportional to \mathbf{B} . We calculate \mathbf{D} , \mathbf{W} , and the corrections to ϵ_d and treat $H_{s.o.}$ and H_{st} as described in Ref. 5.

An important difference in the two cases is that here \mathbf{A} is a function of y so that $f(r)$ is not a plane wave. Instead, we have

$$f_d(r) = \frac{e^{i(k_x x + k_z z)}}{\sqrt{N_{XZ}}} F_d(y), \quad (7)$$

where $F_d(y)$ is a function of y which must be determined and N_{XZ} is the number of zinc-blende unit cells in the X - Z plane of the superlattice. As in the usual treatment of bulk semiconductors in a magnetic field,¹⁻⁴ the functions $F_d(y)$ are expanded in terms of harmonic-oscillator eigenstates. We define harmonic-oscillator creation and destruction operators by

$$a^\dagger = \left[\frac{\hbar}{2\omega m} \right]^{1/2} \left[- \left[k_x - \frac{eB}{\hbar c} y \right] - \frac{i}{\hbar} P_y \right], \quad (8a)$$

$$a = \left[\frac{\hbar}{2\omega m} \right]^{1/2} \left[- \left[k_x - \frac{eB}{\hbar c} y \right] + \frac{i}{\hbar} P_y \right], \quad (8b)$$

where

$$\omega = \frac{eB}{mc}. \quad (8c)$$

The wave vector k_x just shifts the origin of the harmonic oscillator eigenfunctions to

$$y' = y - \frac{\hbar}{m\omega} k_x. \quad (9)$$

We transform to a Kramers' basis defined by

$$|1\rangle = |S\uparrow\rangle, \quad (10a)$$

$$|2\rangle = |S\downarrow\rangle, \quad (10b)$$

$$|3\rangle = \left|\frac{3}{2}\frac{3}{2}\right\rangle = \frac{1}{\sqrt{2}}|(X+iY)\uparrow\rangle, \quad (10c)$$

$$|4\rangle = \left|\frac{3}{2}-\frac{3}{2}\right\rangle = \frac{1}{\sqrt{2}}|(X-iY)\downarrow\rangle, \quad (10d)$$

$$|5\rangle = \left|\frac{3}{2}-\frac{1}{2}\right\rangle = \frac{1}{\sqrt{6}}|2Z\downarrow + (X-iY)\uparrow\rangle, \quad (10e)$$

$$|6\rangle = \left|\frac{3}{2}\frac{1}{2}\right\rangle = \frac{1}{\sqrt{6}}|2Z\uparrow - (X+iY)\downarrow\rangle, \quad (10f)$$

$$|7\rangle = \left|\frac{1}{2}-\frac{1}{2}\right\rangle = \frac{1}{\sqrt{3}}|Z\downarrow - (X-iY)\uparrow\rangle, \quad (10g)$$

$$|8\rangle = \left|\frac{1}{2}\frac{1}{2}\right\rangle = \frac{1}{\sqrt{3}}|Z\uparrow + (X+iY)\downarrow\rangle, \quad (10h)$$

where $|S\rangle$ is the spatial Γ_1 zone-center state; $|X\rangle$, $|Y\rangle$, and $|Z\rangle$ are the spatial Γ_{15} zone-center states of the reference Hamiltonian and spins are quantized along the z axis.

We rewrite Eq. (5a) as

$$[H_{dd'}^2(k_z)^2 + H_{dd'}^1(k_z) + H_{dd'}^0]C_d F_{d'}(y') = 0, \quad (11)$$

where the energy has been included in H^0 . Equation (11) displays the k_z dependence of the Hamiltonian. We specifically write out the matrices H^2 , H^1 , and H^0 in the Appendix. Note, H^2 is the same for the two constituent materials whereas H^1 and H^0 are different. The value of the wave vector k_x does not enter into Eq. (11) except in defining y' . We drop two classes of terms in Eq. (11): those proportional to the second-order matrix element designated B (Ref. 20) and those proportional to the second-order matrix element $(\gamma'_3 - \gamma'_2)$. (See Appendix.) The first class of terms are often called inversion-asymmetry terms because they vanish in the diamond structure. The second class of terms are often called warping terms. These terms are usually neglected in bulk calculations. Therefore, our neglect of them here is consistent with the goal of describing the superlattice at the same level of approximation as is typically used in bulk calculations.

After these terms have been neglected, Eq. (11) simplifies considerably. By making the replacement

$$C_d^n F_d(y) \rightarrow \begin{bmatrix} C_1^n h_n(y') \\ C_3^n h_{n-1}(y') \\ C_5^n h_{n+1}(y') \\ C_7^n h_{n+1}(y') \\ C_2^n h_{n+1}(y') \\ C_4^n h_{n+2}(y') \\ C_6^n h_n(y') \\ C_8^n h_n(y') \end{bmatrix}, \quad (12)$$

where h_n is the n th harmonic oscillator eigenstate, Eq. (11) reduces to an 8×8 eigenvalue equation for the

coefficients C and the energy E . The operators a^\dagger and a are replaced by c -numbers which depend on the Landau index n .

For complex-band-structure calculations, we fix the energy and the Landau index and find the possible values of k_z . Here n can take on integral values larger than or equal to -2 . The dimension of the matrices H^i depend on the Landau index. For $n = -2$ they are 1×1 matrices. For $n = -1$ they are 4×4 matrices. For $n = 0$ they are 7×7 matrices. For $n \geq 1$ they are 8×8 matrices. As has previously been shown,²¹ the complex-band-structure problem can be written as a linear eigenvalue equation for k_z (from now on we will let k , without a vector sign, refer to the z component of wave vector and \mathbf{k} , with a vector sign, refer to a three-dimensional wave vector),

$$\begin{bmatrix} 0 & 1 \\ -(H^2)^{-1}H^0 & -(H^2)^{-1}H^1 \end{bmatrix} \begin{bmatrix} C \\ kC \end{bmatrix} = k \begin{bmatrix} C \\ kC \end{bmatrix}. \quad (13)$$

In Eq. (13) the Landau index has been fixed and creation and destruction operators replaced by c -numbers. This eigenvalue problem can be solved by standard matrix techniques. The matrix is not Hermitian so that complex values of k , corresponding to the evanescent states, occur. The dimension of the matrix, which corresponds to the number of eigenvalues, depends on the Landau index and is twice the dimension of the H matrices.

The H matrices which appear in Eq. (13) are Hermitian. As shown in Ref. 5, this ensures that if k_j is an eigenvalue of Eq. (13), k_j^* is also an eigenvalue. [We define the label j^* by $k_{j^*} = (k_j)^*$.] Once the second-order momentum matrix element B has been dropped, the Hamiltonian has inversion symmetry. That is, this approximation increases the symmetry of the Hamiltonian to that of a diamond-structure semiconductor. The diamond structure has a symmetry operator which consists of a 180° rotation about the z axis followed by inversion. Because the vector potential is an axial vector, it is also invariant under this symmetry operator. As a result, the Hamiltonian including the magnetic field but with the momentum matrix element B dropped commutes with this operator. Using the same argument that was applied in Ref. 5 for a 180° rotation about the z axis followed by time reversal (time reversal is not a symmetry operator in the presence of the magnetic field) one sees that if k_j is an eigenvalue of Eq. (13), $-k_j$ is also an eigenvalue. Combining with the previous result, we see that if k_j is an eigenvalue of Eq. (13), k_j^* , $-k_j$, and $-k_j^*$ are also eigenvalues.

In Fig. 1 we show the complex band structure of $\text{Ga}_{0.47}\text{In}_{0.53}\text{As}$ for an applied field of 10 T. The $n = -2$, -1 , 0 , and 1 cases are shown. The results are independent of k_x . For each value of k shown, k^* , $-k$, and $-k^*$ are also eigenvalues. The numbers next to each line indicate how many solutions it represents. There is a small "spin" splitting which is not always resolved on the scale in Fig. 1. At every energy there are two solutions for $n = -2$, eight solutions for $n = -1$, 14 solutions for $n = 0$, and 16 solutions for $n \geq 1$.

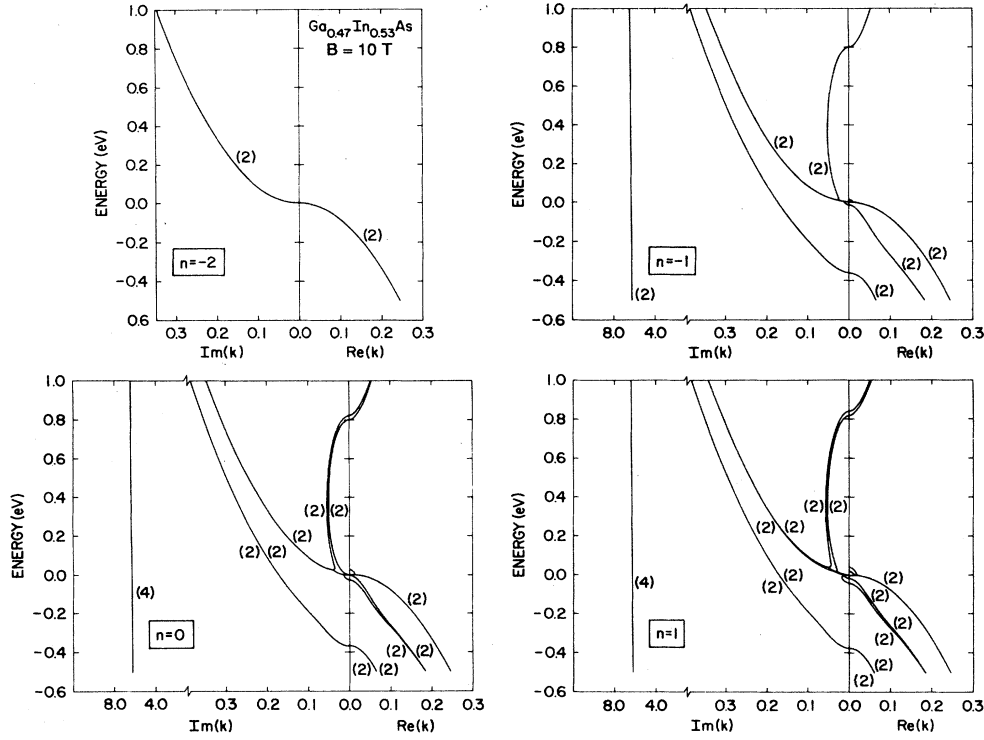


FIG. 1. Complex band structure for $\text{Ga}_{0.47}\text{In}_{0.53}\text{As}$ at $B = 10$ T. Results for the Landau index $n = -2, -1, 0$, and 1 are shown. The number of distinct solutions represented by each line is indicated.

Orthogonality and completeness conditions for the eigenvectors of Eq. (13) play an important role in the superlattice theory. These relations are the same as stated in Ref. 5 and are proved in the same way.

B. Interface description

In the description of the individual materials making up a superlattice, there is an arbitrary energy zero. When describing an interface between two materials, the energy scales of the two materials must be the same. We include an offset energy between the valence-band maxima of the two materials.²² We take this energy offset to be given empirically.

We consider a single interface between two materials and expand the interface eigenstate Ψ , with a given energy, in terms of the individual material bulk eigenstates [that is, the eigenvectors of Eq. (13)] with that value of energy

$$\Psi(r) = \sum_j A_j \psi_j(r) + \sum_i B_i \phi_i(r), \quad (14)$$

where A_j and B_i are expansion coefficients and $\psi_j(\phi_i)$ are the eigenstates in material $a(b)$ with the given energy. In Eq. (14) the interface is assumed abrupt so that r is either in material a or b . The notation in Eq. (14) means that the sum on ψ is taken for r in material a and the sum on ϕ is taken for r in material b .

Without a magnetic field, only states with the same component of wave vector parallel to the interface couple. Thus, only states with a given value of k_{\parallel} are included in the sums of Eq. (14). In Ref. 5 it was shown that the coefficients satisfy

$$A_j = \sum_i \frac{1}{J_{j*}^a} J_{j*}^{ab} B_i \quad (15a)$$

or equivalently

$$B_i = \sum_j \frac{1}{J_{i*}^b} J_{i*}^{ba} A_j. \quad (15b)$$

Here J_{j*}^{ab} is the z component of the current density operator between the state ψ_{j*} which is an eigenstate in material l and ψ_i which is an eigenstate in material l' . The current density operator is evaluated at the origin, which is taken to be on the interface, and averaged over a unit cell. In each constituent material, the orthogonality condition of the eigenvalue equation is

$$J_{j*}^l = J_{j*}^l \delta_{ji}. \quad (16)$$

The completeness conditions of the eigenvalue equations were used to show that

$$\sum_i \frac{1}{J_{j*}^a} J_{j*}^{ab} \frac{1}{J_{i*}^b} J_{i*}^{ba} = \delta_{jj'}. \quad (17)$$

Equation (17) ensures flux conservation at the interface.

The application of a magnetic field parallel to the growth axis changes these results very slightly. We first notice that the bulk quantum number k_x will be conserved at the interface. We next redefine the current density matrices by integrating along the y axis

$$J_{j*}^{II'} \equiv \frac{1}{L} \int dy \langle \psi_{j*} | J_z(x, y, 0) | \psi_{i'} \rangle_A. \quad (18)$$

Here L is the length of the superlattice in the y direction, J_z is evaluated at the interface ($z=0$), the subscript A indicates an average over the unit cell, and the value of x is irrelevant. The vector potential only has a component in the X direction, and therefore it does not make a contribution to J_z . As in Ref. 5 we neglect spin-orbit contributions to the current density operator. These contributions are very small, comparable to k -dependent spin-orbit interaction terms. The integral over y must be performed in order to turn products of the harmonic oscillator functions into matrix elements. Without a magnetic field, the matrix element in Eq. (18) is independent of y and so the integral does not change anything. With this definition, the current density matrices are given by

$$J_{j*}^I = \frac{1}{\hbar\Omega} C_{j*}^{I\dagger} [H^2(k_j^I + k_i^I) + H^{II}] C_i^I \quad (19a)$$

and

$$\begin{aligned} J_{j*}^{II'} &= \frac{1}{\hbar\Omega} C_{j*}^{II'\dagger} [H^2(k_j^{II'} + k_i^{II'}) + H^{II} - \Delta] C_i^{II'} \\ &= \frac{1}{\hbar\Omega} C_{j*}^{II'\dagger} [H^2(k_j^{II'} + k_i^{II'}) + H^{II'} + \Delta^\dagger] C_i^{II'}, \end{aligned} \quad (19b)$$

where

$$\Delta_{dd'} = 2 \sum_{\beta} \frac{\langle U_d | P_z | U_{\beta} \rangle \langle U_{\beta} | \Delta V^I | U_{d'} \rangle}{(\epsilon_d + \epsilon_{d'}/2) - \epsilon_{\beta}}. \quad (19c)$$

These results have the same structure as in Ref. 5 and are derived in the same way. The term H^2 does not mix states with different Landau indices. After the matrix element B has been dropped, as was already done so that the Landau index would be a good quantum number in the bulk, the term H^I does not mix states with different Landau indices. It is also necessary to drop the term $\Delta_{xy} = \Delta_{yx}$ in Eq. (19b) to avoid mixing Landau indices. This term is generally small. It vanishes exactly for diamond-structure materials. Thus, it is an inversion-asymmetry term like the matrix element B and dropping it is analogous to dropping this matrix element. With this additional approximation, the current density matrices are all diagonal in the Landau index.

The results from Ref. 5, stated above, now all follow by the same arguments given there. Equation (16) is the orthogonality condition of Eq. (13). Equation (17) follows from the completeness conditions of Eq. (13). Equation (15) is the interface matching conditions, and Eq. (17) ensures flux conservation.

C. Superlattice eigenvalue equation

The superlattice translational symmetry in the z direction is used to derive the superlattice eigenvalue equation

exactly as in Ref. 5 without the magnetic field. This equation reads

$$\sum_{j'} M_{jj'} A_{j'} = e^{iQ(\alpha+\beta)} A_j, \quad (20a)$$

$$M_{jj'} = \sum_i e^{ik_j^a \alpha} \frac{1}{J_{j*}^a} J_{j*}^{ab} e^{ik_i^b \beta} \frac{1}{J_{i*}^b} J_{i*}^{ba}, \quad (20b)$$

where Q is the superlattice wave vector in the z direction, A_j are expansion coefficients of the states ψ_j in material a , and α and β are the layer thicknesses of material a and b . The expansion coefficients of the states ϕ_j in material b are given by the same relations as in Ref. 5. The other results of Sec. IV in Ref. 5 follow without modification except for the argument which relies on time reversal invariance. In this case, as in the bulk argument, we use a combination of a 180° rotation about the z axis and inversion (which becomes a symmetry of the problem since all the inversion-asymmetry terms have been dropped) to show that if Q is a superlattice wave vector $-Q$ is also. Combined with the unmodified argument of Ref. 5, which shows that if Q is a superlattice wave vector Q^* is also, we have that Q , Q^* , $-Q$, and $-Q^*$ came together as superlattice wave vectors.

Thus, the formal approach in the presence of an applied magnetic field along the growth axis is similar to that without a magnetic field. The differences are that the Hamiltonian takes a different form. The quantum numbers in the complex-band-structure calculations are k_x , n , and E rather than k_x , k_y , and E . It was necessary to drop the inversion-asymmetry and warping terms in order to have n a quantum number. Time reversal symmetry is lost, but with the neglect of the inversion-asymmetry terms spatial inversion becomes a symmetry. Many of the results that follow from time reversal without the magnetic field now follow from spatial inversion.

We have specifically considered [001] growth axis superlattices with the magnetic field applied along the growth axis. It is relatively straightforward to consider other growth orientations. It is not straightforward to consider cases where the magnetic field is not along the growth axis.

III. NUMERICAL RESULTS

In this section we present the results of numerical calculations of the electronic structure of a nonmagnetic superlattice and a semimagnetic superlattice. We use the formal results of the previous section. It is necessary to treat $n = -2$, -1 , and 0 as special cases because the matrices have smaller dimension than for the general case. The numerical implementation of the formal results follows the discussion of Ref. 6. In particular, the results of the Appendix, which shows how to handle states with large values of $|\text{Im}k|$, are unmodified by the magnetic field.

We first consider the nonmagnetic superlattice $\text{Ga}_{0.47}\text{In}_{0.53}\text{As}/\text{Al}_{0.48}\text{In}_{0.52}\text{As}$. The lattice constants of the constituent materials in the superlattice are matched to each other and to an InP substrate. Therefore, there is

no strain or exchange contribution to the Hamiltonian. Electronic structure calculations without a magnetic field are presented for this superlattice in Ref. 6. We calculate the various momentum matrix elements and energy shifts using a reference pseudopotential as discussed there. We set the second-order matrix element B , the warping constant $(\gamma'_3 - \gamma'_2)$, and the parameter Δ_{xy} to zero. The valence-band offset, spin-orbit splitting, and other empirical parameters are the same as Ref. 6.

In Fig. 2 we show the calculated energy positions for the first conduction-band level C_1 , the first heavy-hole level HH_1 , and the first light-hole level LH_1 , for a superlattice consisting of 12 molecular layers of $\text{Ga}_{0.47}\text{In}_{0.53}\text{As}$ and 12 molecular layers of $\text{Al}_{0.48}\text{In}_{0.52}\text{As}$ as a function of magnetic field strength. Results for Landau indices $-2 \leq n \leq 2$ are shown. The superlattice wave vector Q is zero. The value of k_x does not enter into calculation. One sees a single $n = -2$ state which is heavy-hole-like. There are three $n = -1$ states, one of each type. There are five $n = 0$ states: two conduction states, one heavy-hole state, and two light-hole states. For $n \geq 1$, there are two states of each type. For the electron states, the splitting between states with different harmonic oscillator functions [see Eq. (12)] is relatively large whereas the splitting between states with the same harmonic oscillator function and different spins is much smaller. For holes, the mixing between the various hole terms in Eq. (11) is quite strong, and the splitting is intermediate between that of the different electron harmonic oscillator functions and different electron spins.

In Fig. 3 we show the energy dispersion relations for the same superlattice as in Fig. 2 at a field of 5 T. The cases $-1 \leq n \leq 2$ are considered. For $n = -2$, only heavy-hole bands, which are essentially dispersionless, occur. The $Q = 0$ point in Fig. 3 corresponds to the $B = 5$ T point in Fig. 2.

We next consider the semimagnetic superlattice $\text{Hg}_{0.95}\text{Mn}_{0.05}\text{Te}/\text{Cd}_{0.78}\text{Mn}_{0.22}\text{Te}$. The lattice constants of the constituent materials are matched to each other so there is no strain contribution to the Hamiltonian. MnTe does not occur in the zinc-blend crystal structure and pseudopotential form factors for a zinc-blend MnTe model are not available. Therefore, we take the momentum matrix elements and band gaps to be empirically given rather than calculating them as was done for $\text{GaInAs}/\text{AlInAs}$. Momentum matrix elements and spin-orbit interaction parameters are taken to be the same in the two constituents and to be equal to those of CdTe given in Ref. 23. The band gaps of the constituent materials are from Refs. 13 and 14. The valence-band offset is taken to be zero. Parameters describing the average spin state of Mn^{2+} ions as a function of magnetic field and temperature are taken from Refs. 24 and 25. The exchange matrix elements are also from Refs. 24 and 25. We assume that these matrix elements and spin parameters are the same in the layers forming the superlattice as they are in the corresponding bulk alloys.

In Fig. 4 we show the calculated energy positions for the first conduction-band level C_1 , the first and second heavy-hole level HH_1 and HH_2 , and the first light-hole

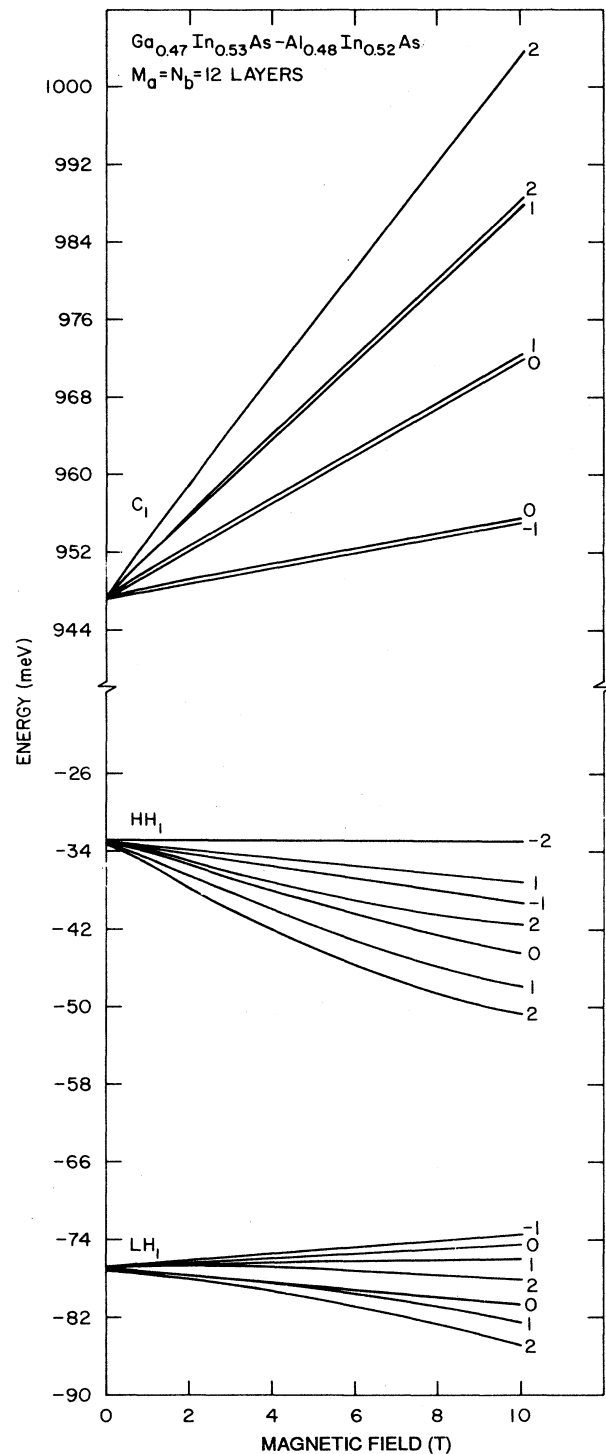


FIG. 2. The first conduction C_1 , first heavy-hole HH_1 , and first light-hole LH_1 energies at the superlattice zone center as a function of magnetic field for a $\text{Ga}_{0.47}\text{In}_{0.53}\text{As}/\text{Al}_{0.48}\text{In}_{0.52}\text{As}$ superlattice consisting of 12 molecular layers of each constituent material. Results are shown for the Landau index $n = -2, -1, 0, 1$, and 2 .

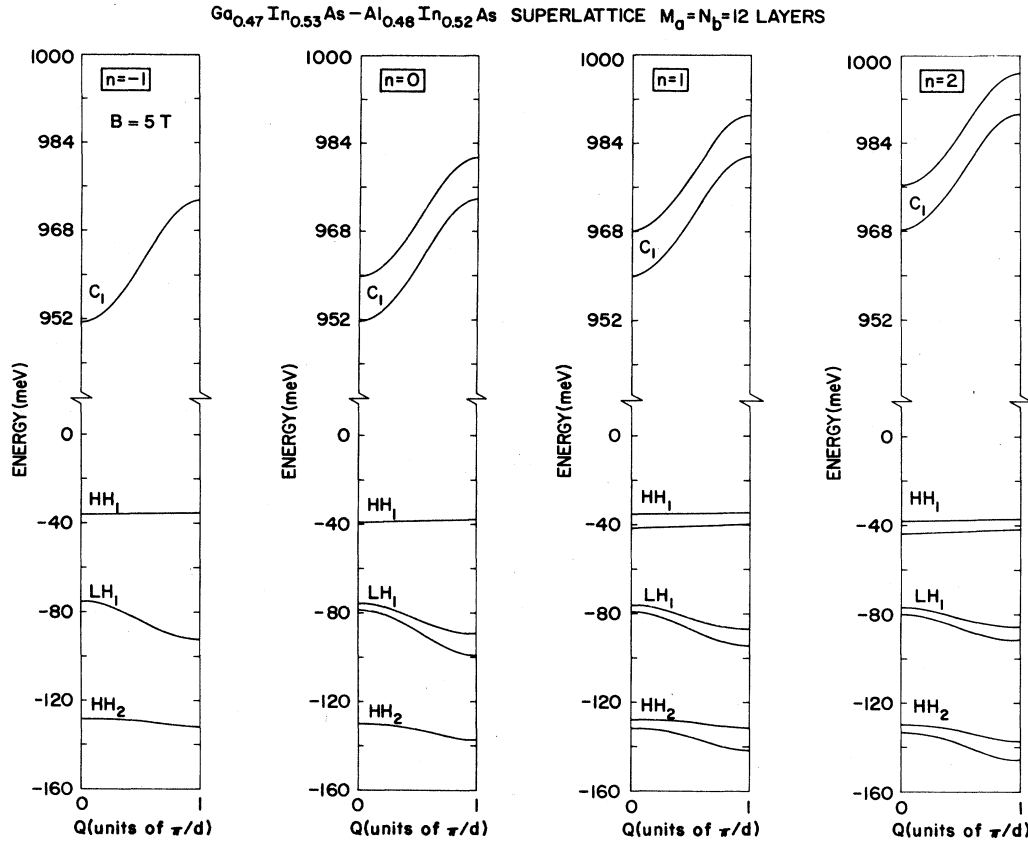


FIG. 3. Energy dispersion curves at $B=5$ T for the same superlattice as in Fig. 2. Results are shown for the Landau index $n = -1, 0, 1$, and 2 .

level LH_1 for a superlattice consisting of four molecular layers of $\text{Hg}_{0.95}\text{Mn}_{0.05}\text{Te}$ and four molecular layers of $\text{Cd}_{0.78}\text{Mn}_{0.22}\text{Te}$ as a function of magnetic field strength. Results for Landau indices $-2 \leq n \leq 2$ are shown. The superlattice wave vector Q is zero. The temperature is zero. The state counting is the same as for the nonmagnetic superlattice of Fig. 2. However, the sizes of the splittings are quite different than in Fig. 2. The exchange interaction has greatly increased the size of the effective spin splitting and the orbital motion splittings are now comparable. For holes, where the exchange integrals are much larger than for electrons, the effective spin splitting is much larger than the orbital motion splitting.

In Fig. 5 we show the energy dispersion relations for the same superlattice as in Fig. 4 at zero temperature and a field of 10 T. The cases $-1 \leq n \leq 2$ are considered. For $n = -2$ only heavy-hole bands, which are essentially dispersionless, occur. The $Q=0$ point in Fig. 5 corresponds to the $B=10$ T point in Fig. 4. There is substantial dispersion because the superlattice layers are quite thin. Strong anticrossing occurs between heavy- and light-hole states.

IV. SUMMARY

We have presented a theory of the electronic structure of direct-band-gap semiconductor superlattices with an applied magnetic field along the growth axis. The theory is based on the $(\mathbf{k} \cdot \mathbf{p})$ formalism and is a generalization of the results of Ref. 5 to include the presence of the magnetic field. We have applied the theory to a nonmagnetic and a semimagnetic superlattice.

ACKNOWLEDGMENT

Two of the authors (G.Y.W. and T.C.M.) would like to acknowledge the support of the Defense Advanced Research Projects Agency monitored by the U.S. Office of Naval Research Under Contract No. ONR-N00014-86-K-0841. The work of D.L.S. was supported by Los Alamos National Laboratory Internal Supporting Research.

APPENDIX: THE HAMILTONIAN

In this appendix we write out the matrices H^2 , H^1 , and H^0 in Eq. (11). We write them in the $|S\rangle$, $|X\rangle$, $|Y\rangle$, $|Z\rangle$

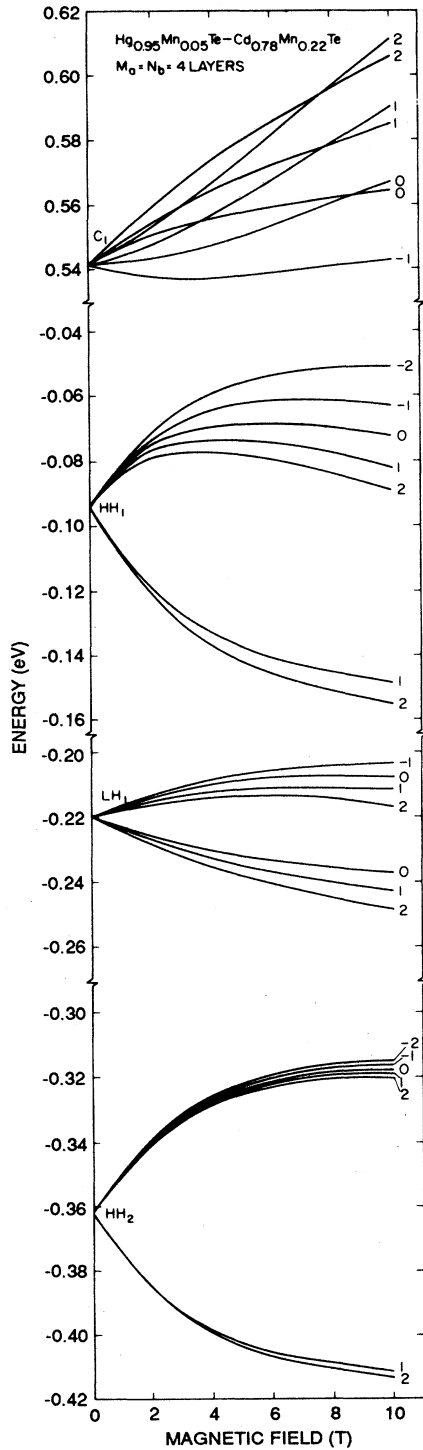


FIG. 4. The first conduction C_1 , first and second heavy-hole HH_1 and HH_2 , and first light-hole LH_1 energies at the superlattice zone center as a function of magnetic field for a $Hg_{0.95}Mn_{0.05}Te/Cd_{0.78}Mn_{0.22}Te$ superlattice consisting of four molecular layers of each constituent material. Results are shown for the Landau index $n = -2, -1, 0, 1$, and 2 at zero temperature.

basis because they can be stated much more compactly in this basis. For actual calculation it is more convenient to use a Kramer's basis such as that defined in Eq. (10). Transformation to the Kramer's basis is straightforward.

It is convenient to write H^0 as the sum of five terms

$$H^0 = H_{s.o.} + H_{st} + H_S + H_\epsilon + H_R^0, \quad (A1)$$

where $H_{s.o.}$ is the spin-orbit interaction, H_{st} is the strain interaction in a strained-layer superlattice, H_S describes the direct coupling of the magnetic field to electron spins, H_ϵ is the exchange interaction, and H_R^0 represents the other contributions.

The matrices H^2 , $H_{s.o.}$ and H_{st} are not affected by the magnetic field and are the same as given in Ref. 5. The matrix H^1 is spin diagonal and independent. Its nonzero matrix elements (we do not write terms related by conjugation for these Hermitian matrices) are

$$(S|Z) = iP^I, \quad (A2a)$$

$$(S|X) = BK_y, \quad (A2b)$$

$$(S|Y) = BK_x, \quad (A2c)$$

$$(X|Z) = N'K_x, \quad (A2d)$$

$$(Y|Z) = N'K_y, \quad (A2e)$$

where

$$P^I = P + \Delta P^I \quad (A2f)$$

and the operators K are given by Eq. (2) and are related to the harmonic-oscillator creation and destruction operators by Eq. (8). The momentum matrix elements are as defined in Ref. 5. H^1 is different for the two constituent materials between ΔP^I depends on the material.

With the virtual-crystal approximation and mean field treatment of Eq. (6), H_ϵ has the same form as H_S and we treat them together. We have

$$H_S + H_\epsilon = \left[\frac{e\hbar}{2mc} B + x \left[\sum_i J(r - R_i) \right] \langle S_Z \rangle \right] \sigma_Z. \quad (A3)$$

The sum on exchange terms has Γ_1 symmetry so that it does not mix states. Defining

$$A_S = \left[\frac{e\hbar}{2mc} B + x \left\langle S \left| \sum_i J(r - R_i) \right| S \right\rangle \langle S_Z \rangle \right] \quad (A4a)$$

and

$$A_P = \left[\frac{e\hbar}{2mc} B + x \left\langle X \left| \sum_i J(r - R_i) \right| X \right\rangle \langle S_Z \rangle \right], \quad (A4b)$$

the nonzero matrix elements of $H_S + H_\epsilon$ are

$$(S\sigma|S\sigma) = \pm A_S, \quad (A5a)$$

$$(X\sigma|X\sigma) = (Y\sigma|Y\sigma) = (Z\sigma|Z\sigma) = \pm A_P. \quad (A5b)$$

In Eqs. (A5), we have the $+$ sign for $\sigma = \uparrow$ and the $-$ sign for $\sigma = \downarrow$. A_S and A_P depend on temperature, concentration, and magnetic field. Parametrized values are

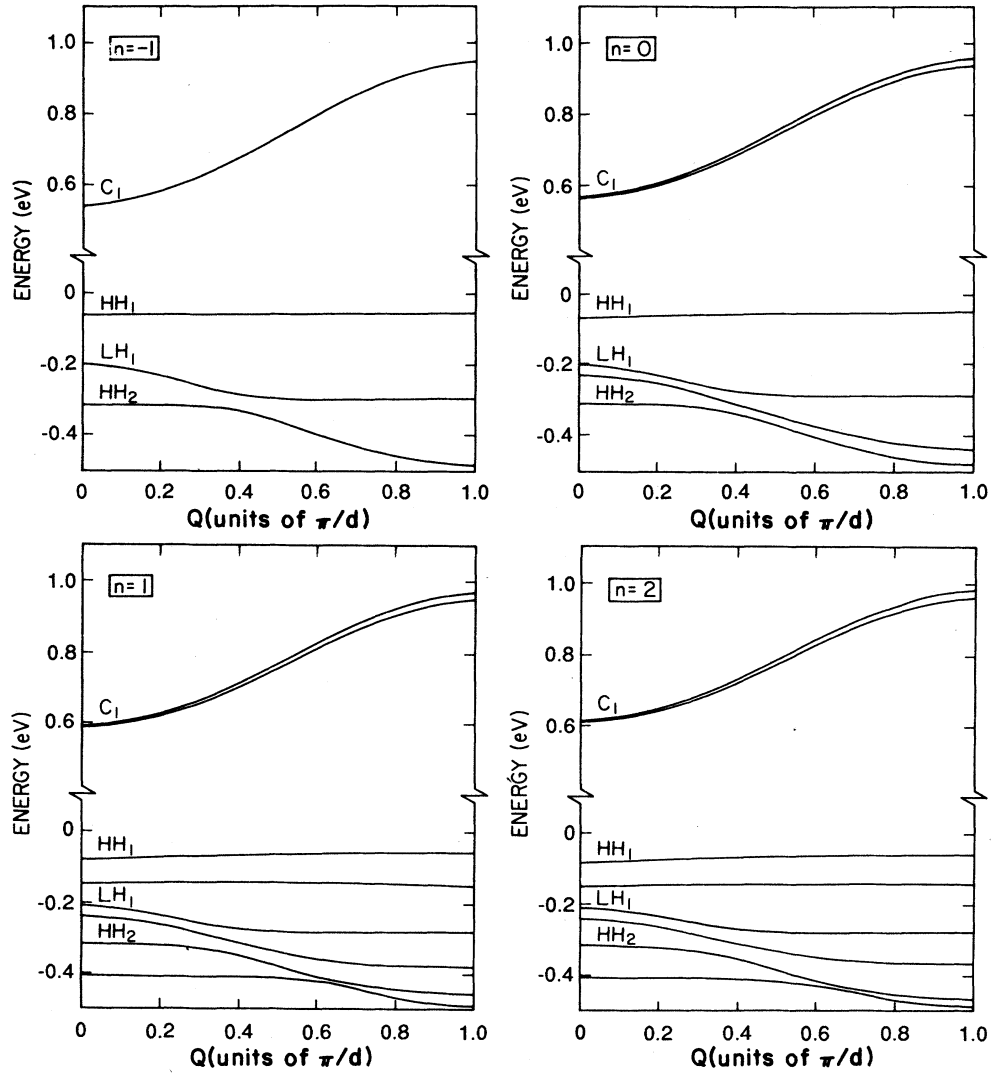


FIG. 5. Energy dispersion curves at $B = 10$ T for the same superlattice as in Fig. 4. Results are shown for the Landau index $n = -1, 0, 1$, and 2 at zero temperature.

given in Refs. 24 and 25.

The matrix H_R^0 is spin diagonal and independent. The nonzero values of H_R^0 (we do not write terms related by conjugation) are

$$(S|S) = (\epsilon_c + \Delta\epsilon_c^I - E) + \left[A' + \frac{\hbar^2}{2m} \right] (K_x^2 + K_y^2), \quad (\text{A6a})$$

$$(X|X) = (\epsilon_v + \Delta\epsilon_v^I - E) + \left[L' + \frac{\hbar^2}{2m} \right] K_x^2 + \left[M + \frac{\hbar^2}{2m} \right] K_y^2, \quad (\text{A6b})$$

$$(Y|Y) = (\epsilon_v + \Delta\epsilon_v^I - E) + \left[M + \frac{\hbar^2}{2m} \right] K_x^2 + \left[L' + \frac{\hbar^2}{2m} \right] K_y^2, \quad (\text{A6c})$$

$$(Z|Z) = (\epsilon_v + \Delta\epsilon_v^I - E) + \left[M + \frac{\hbar^2}{2m} \right] (K_x^2 + K_y^2), \quad (\text{A6d})$$

$$(S|X) = iP^I K_x, \quad (\text{A6e})$$

$$(S|Y) = iP^I K_y, \quad (\text{A6f})$$

$$(S|Z) = \frac{1}{2}B(K_x K_y + K_y K_x), \quad (\text{A6g})$$

$$(X|Y) = (F' - G)K_x K_y + (H_1 - H_2)K_y K_x. \quad (\text{A6h})$$

The operators K_x and K_y do not commute. The momentum matrix elements are as defined in Ref. 5. H_R^0 is different in the two constituent materials because ΔP^I , $\Delta \epsilon_c^I$, and $\Delta \epsilon_v^I$ are different in the two constituent materials. In order to have the Landau index a good quantum number, it is necessary to drop the inversion-symmetry matrix element B and warping terms proportional to

$$(\gamma'_3 - \gamma'_2) = \frac{2m}{\hbar^2} \frac{1}{6} (L' - M - N'). \quad (\text{A7})$$

The warping terms come into H_R^0 from some combinations of the terms proportional to K^2 in Eq. (A6) when the transformation to the Kramer's basis is made.

*Present address: Department of Physics, Harvard University, Cambridge, MA 02138.

¹C. R. Pidgeon and R. N. Brown, Phys. Rev. **146**, 575 (1966).

²W. Leung and L. Liu, Phys. Rev. **138**, 3811 (1973).

³M. H. Weiler, R. L. Aggarwal, and B. Lax, Phys. Rev. B **17**, 3269 (1978).

⁴R. L. Aggarwal, in *Semiconductors and Semimetals*, edited by R. K. Willardson and A. C. Beer (Academic, New York, 1972), Vol. 9, p. 151.

⁵D. L. Smith and C. Mailhot, Phys. Rev. B **33**, 8345 (1986).

⁶C. Mailhot and D. L. Smith, Phys. Rev. B **33**, 8360 (1986).

⁷A. Fasolino and M. Altarelli, in *Two-Dimensional Systems: Heterostructures and Superlattices*, edited by G. Bauer, F. Kuchar, and H. Heinrich (Springer, Berlin, 1984), p. 176.

⁸A. Fasolino and M. Altarelli, Surf. Sci. **142**, 322 (1984).

⁹G. Bastard and J. A. Brum, IEEE J. Quantum Electron. **QE-22**, 1625 (1986).

¹⁰S. Lamari and L. J. Sham, Surf. Sci. **196**, 551 (1988).

¹¹J. C. Maan, Surf. Sci. **196**, 518 (1988).

¹²J. A. Brum, P. Voisin, M. Voos, L. L. Chang, and L. Esaki, Surf. Sci. **196**, 545 (1988).

¹³N. B. Brandt and V. V. Moshchalkov, Adv. Phys. **33**, 193 (1984).

¹⁴J. K. Furdyna, J. Appl. Phys. **53**, 7637 (1982).

¹⁵G. Y. Wu, D. L. Smith, C. Mailhot, and T. C. McGill, Appl. Phys. Lett. **49**, 1551 (1986).

¹⁶G. Y. Wu, T. C. McGill, D. L. Smith, and C. Mailhot, J. Vac. Sci. Technol. A **5**, 3096 (1987).

¹⁷P.-O. Löwdin, J. Chem. Phys. **19**, 1396 (1951).

¹⁸We neglect interband mixing by the magnetic field.

¹⁹We neglect the k dependence of the spin-orbit and stress interaction.

²⁰E. O. Kane, in *Semiconductors and Semimetals*, edited by R. K. Willardson and A. C. Beer (Academic, New York, 1966), Vol. 1, p. 75.

²¹Y. C. Chang and J. N. Schulman, Phys. Rev. B **25**, 3975 (1982).

²²See, for example, H. Kroemer, in *Proceedings of the NATO Advanced Study Institute on Molecular Beam Epitaxy and Heterostructures, Erice, Sicily, 1983*, edited by L. L. Chang and K. Ploog (Nijhoff, Leyden, 1985), p. 331.

²³P. Lawaetz, Phys. Rev. B **10**, 3460 (1971).

²⁴J. A. Gaj, R. Planel, and G. Fishman, Solid State Commun. **29**, 435 (1970).

²⁵I. I. Lyapilin and I. M. Tsiril'kovskii, Usp. Fiz. Nauk **146**, 35 (1985) [Sov. Phys.—Usp. **28**, 349 (1985)].